ELSEVIER

Ceramics International 30 (2004) 1003–1008

CERAMICS INTERNATIONAL

www.elsevier.com/locate/ceramint

Sintering effects on dielectric properties of (Ba,Sr)TiO_3 ceramics

L. Szymczak*, Z. Ujma, J. Hañderek, J. Kapusta

Institute of Physics, University of Silesia, ul. Uniwersytecka 4, 40-007 Katowice, Poland

Received 2 April 2003; received in revised form 19 September 2003; accepted 22 October 2003

Available online 3 April 2004

Abstract

The sintering effect on transition parameters and dielectric characteristics of $Ba_{0.8}Sr_{0.2}TiO_3$ (BST 80/20) ceramics prepared by the conventional mixed-oxide processing technique was studied. Grain structure analysis performed by a scanning electron microscope (SEM) and X-ray diffraction studies showed differences in grain size and contents of crystal phase within the ceramics sintered at constant temperature for a variety of sintering times. The phase transitions and dielectric properties were investigated by measuring the dielectric constant ε', the loss factor tan δ and the remanent polarization P_r as a function of temperature. The frequency dependence of $\varepsilon'(T)$ and tan $\delta(T)$ characteristics was also studied. It was shown that the maximal values of the dielectric constant and the remanent polarization are in general proportional to the content of the crystal phase in the volume of the studied ceramics.

Keywords: B. X-ray methods; C. Dielectric properties; Ferroelectricity; Ceramics; Oxides

1. Introduction

Barium–strontium titanate (BST) ceramics have been widely studied due to their potential application in microwave devices. Their properties have been reported in a number of papers, cited among others in ref. [1–4] and so has the influence of grain size on the parameters of ferroelectric phase transitions and dielectric characteristics [5–11]. Up till now the grain-size effects have been investigated for a number of ferroelectric ceramics prepared with the use of the conventional mixed-oxide processing technique with selected conditions of the sintering process [7,9,12], with the use of different methods of ceramics [8] or by thin film preparation [5,6,10,13–15]. The grain-size effect was studied both experimentally [5–15] and theoretically [16,17]. Some authors not only predicted theoretically but also observed experimentally the rise of values of ε'_{max} and corresponding temperature T_m with the increase of grain size [5,6,13–15]. On the other hand, the lowering of T_m was also observed and described [9,11,12,15]. Such behaviour was also found in BST ceramics with relatively large grains [9,11]. The reweave of various interpretation models is presented in paper [12]. It is worthwhile, however, to mention that some differences in the experimental data on the grain-size effect in BST ceramics with different grain structure contradict each other [9,11] and have not yet been fully explained.

An interpretation of the experimental data reported in our paper takes into consideration certain factors sometimes omitted in earlier papers. We attempt to explain the observed differences in dielectric characteristics by the influence of the internal mechanical stress and local electric fields associated with the non-homogeneous distribution of ion defects, and especially oxygen vacancies.

2. Ceramics preparation and their grain structure

The $(Ba_{0.8}Sr_{0.2})TiO_3$ ceramics with various grain size were prepared using the conventional mixed-oxide processing technique. Stoichiometric amounts of $BaCO_3$, $SrCO_3$ and TiO_2 oxides were weighed and mixed. Thermal synthesis of the pressed mixture was carried out at $T_S = 925\,^{\circ}C$ for $t_S = 4\,h$. Then the crushed, milled and sieved materials were pressed again into cylindrical pellets and sintered at $T_S = 1250\,^{\circ}C$ for $t_S = 4\,h$. The latter procedure was repeated before the final sintering, carried out at $T_S = 1460\,^{\circ}C$ constant for each sintered ceramics, however, for various

* Corresponding author. Tel.: +48-32-2588211; fax: +48-32-2588431.
E-mail address: lszymcza@us.edu.pl (L. Szymczak).

0272-8842/$30.00
doi:10.1016/j.ceramint.2003.10.019

Table 1
Average grain size and relative density for BST 80/20 ceramics with various sintering conditions

	Sintering conditions			
	t_S (T_S = 1460 °C)			
	1 h	3 h	4 h	7 h
Relative density (%)	87.3	87.1	95.1	95.7
Average grain size (μm)	24.9	31.2	35.6	44.2

sintering times given in Table 1. It is worthwhile to stress that some authors studied the BST ceramics with a different grain structure obtained by a selection of the sintering temperature [5,6,8]. Hence, these materials could differ significantly in the concentration of ion defects, which is strongly temperature-dependent.

The Archimedes displacement method with distilled water was employed to evaluate sample density. Densities of BST 80/20 ceramics obtained for various sintering conditions are given in Table 1. Increase of the sintering time at 1460 °C leads to higher density of the obtained ceramics. The densification process reaches its maximum for the sintering time $t_S \cong 7$ h. The experimental results show that this sintering time makes it possible to obtain ceramics with optimum dielectric properties. Further increase of the sintering time leads to the worsening of these properties. This is probably caused by the increase of the defect concentration.

The scanning electron microscope JSM-5410 with energy dispersion X-ray spectrometer (EDS) was used for investigation of the grain structure and to control the distribution of individual elements within the grains. The grain-size measurements were performed on the fracture surface of the ceramics. Images of the microstructure of the BST 80/20 ceramics for various sintering times are shown in Fig. 1. The average grain size determined by statistical analysis of the SEM measurements is given in Table 1. As can be expected grains grow with the increase of the sintering time. It is also shown that with the rise of the sintering time a more complicated mixture of grain size occurs. In the samples sintered for a longer time up to 7 h large grains from 20 to 60 μm in size are formed in a matrix of smaller grains. Similar results were obtained by authors of paper [7].

Energy dispersion X-ray spectrometer was used to check the distribution of individual elements within the grains. The EDS analysis indicates a fairly homogenous distribution of these elements throughout the grains. Moreover, the quantitative microanalysis with the implementation of SEMQuant programs elaborated by Oxford Instruments (Link "ISIS" Series 300 system), shows that the content of Sr is almost identical when scanning is performed along the individual grains and along the surfaces of the fracture of the ceramics obtained for different sintering times. Differences in the Sr content do not exceed 0.1 atomic percent. The more significant differences, reaching even a few at.%, were observed in the oxygen content. As could be expected, the ceramics

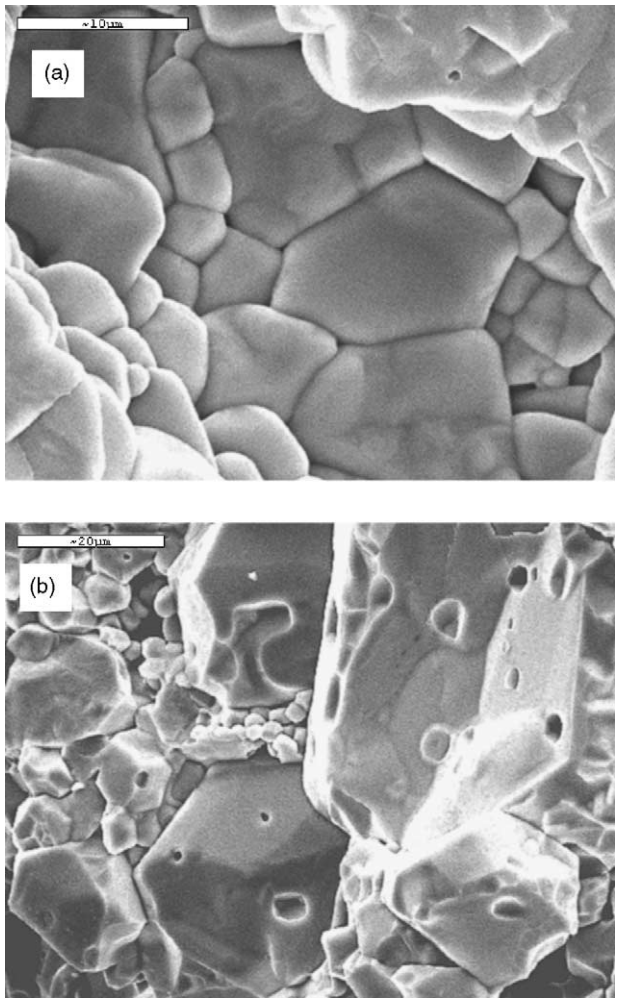

Fig. 1. SEM images of the fracture surface of BST 80/20 sintered at T_S = 1460 °C for 4 h (a) and 7 h (b).

sintered for 7 h shows lower content of the oxygen in comparison with ceramics sintered for 1 h. This is the consequence of the oxygen reduction process, which is strongly temperature and sintering time dependent.

The X-ray diffraction patterns (XRD) of $BaTiO_3$ and BST 80/20 obtained at room temperature at various sintering times t_S are shown in Fig. 2. XRD measurements were carried out on powdered samples using a high resolution Siemens diffractometer (θ–θ) D 5000 with filtered Cu Kα radiation (40 kV, 30 mA). The powder diffraction diagrams (Fig. 2) were measured from 10 to 100° in 2θ with 0.02° steps and a 2 s counting time. XRD patterns show that the crystal structures exhibit tetragonal symmetry at room temperature (space group *P*4*mm*) for all the studied BST ceramics. In all of them a single phase, isostructural perovskite solid solutions, is observed. No reflections associated with the $SrTiO_3$ were found. The lattice parameters obtained from the X-ray patterns were a = 3.9783 Å and c = 3.9930 Å (tetragonal distortion c/a = 1.004) for BST 80/20 ceramics sintered at T_S = 1460° for t_S = 7 h. One can assume that the increase in diffraction maxima (Fig. 2), observed

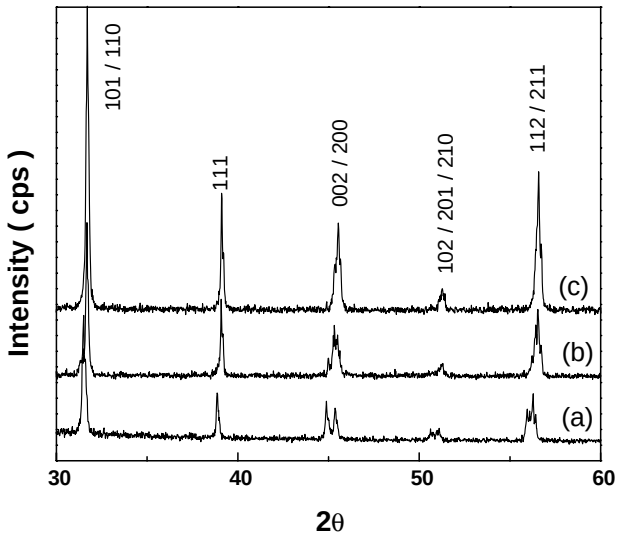

Fig. 2. Part of the diffraction patterns of the $BaTiO_3$ (a) and BST 80/20 sintered at $T_S = 1460\,^{\circ}C$ for 1 h (b) and 7 h (c).

for the BST 80/20 ceramics, obtained with rising sintering time, is caused by a different content of the crystal phase in the ceramics. It is evident that a small-grained sample ($t_S =$ 1 h) contains a more amorphous phase within the notably more developed total grain boundary (Fig. 1). Relation of the integrated diffraction maxima for the ceramics sintered for 1 and 7 h amount to about 2.5. One can assume that the small-grained ceramics contain a considerably less crystal phase in its volume.

3. Dielectric measurements

The cut and polished 0.6 mm thick samples, coated with silver electrodes, were used for the measurements of the dielectric constant (ε') and the loss factor ($\tan\delta$) as a function of temperature. An automatic measuring system with HP 4192A impedance analyser was used to measure and record ε' and $\tan\delta$ numerically. Some characteristics $\varepsilon'(T)$ and $\tan\delta(T)$ obtained on heating at the measuring field of frequency 1 kHz, for ceramics sintered at $T_S = 1460\,^{\circ}C$ for various sintering times are shown in Fig. 3. Both $\varepsilon'(T)$ and $\tan\delta(T)$ curves reveal anomalies in the vicinities of temperatures corresponding to the orthorhombic–tetragonal ($F_O - F_T$) and tetragonal–cubic ($F_T - P_C$) phase transitions, respectively. It is noteworthy that ε'_{max} increases and the corresponding temperature $T_m \equiv T_{F_T-P_C}$ decreases with the increase of the sintering time up to $t_S = 7$ h and associated increase of average grain size (Fig. 4). The peaks on the $\varepsilon'(T)$ curves are diffused for all the studied ceramics. Deviations from the Curie–Weiss law were observed in the range of the paraelectric phase. These deviations can be described by the parameter γ in the formula $1/\varepsilon' - 1/\varepsilon'_{max} = C/(T - T_{max})^{\gamma}$. The determined diffuseness exponent γ versus sintering time is shown in Fig. 3.

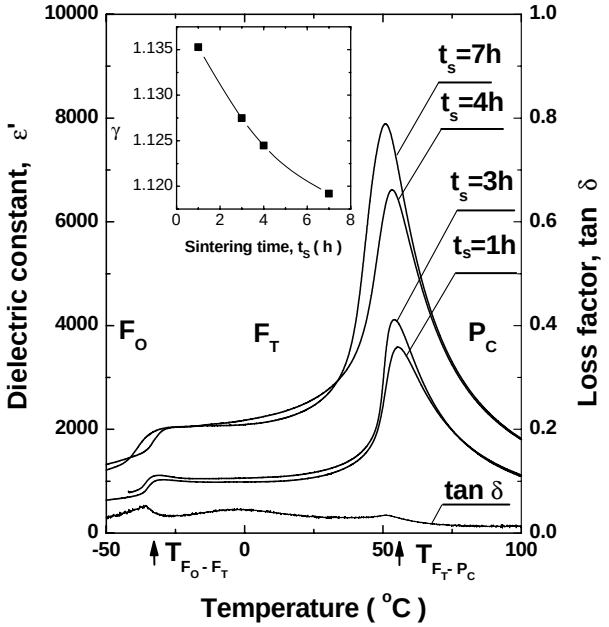

Fig. 3. Dielectric constant as a function of temperature, measured on heating at frequency of measuring field 1 kHz for ceramics with different sintering time. Diffuseness exponent γ vs. the sintering time is shown in the inserted figure. The example of loss factor vs. temperature, measured for ceramics sintered for 1 h, is also shown in the figure.

The characteristics $\varepsilon'(T)$ for a number of frequencies of the measuring field are shown in Fig. 5 for the ceramics sintered at $T_S = 1460\,^{\circ}C$ for $t_S = 1$ h and $t_S = 7$ h. The ε'_{max} is strongly dependent on the frequency of the electric field applied to both these ceramics (Figs. 5 and 6), whereas the temperatures T_m corresponding to these maxima are weakly dependent on the frequency (Fig. 6). The

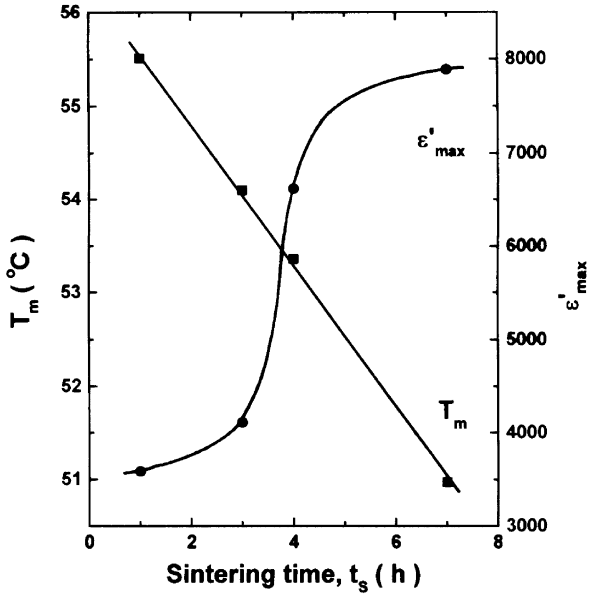

Fig. 4. The maxima in $\epsilon'(T)$ curves and corresponding temperatures T_m as a function of sintering time t_S for ceramics sintered at $T_S = 1460\,^{\circ}C$.

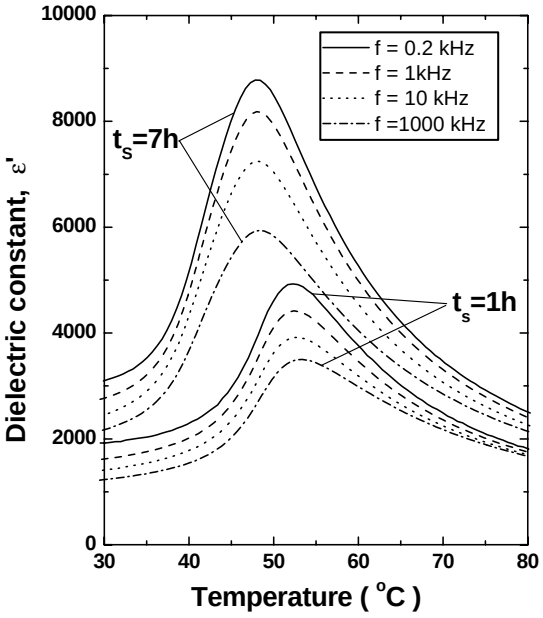

Fig. 5. The temperature dependence of ε' for ceramics sintered at $T_S = 1460\,^{\circ}C$ with different sintering time t_S for four various frequencies of measuring field.

frequency dependence of ε'_{max} is relatively more distinct for the ceramics sintered for $t_S = 7\,h$.

The investigated BST 80/20 ceramics show additional anomalies in $\varepsilon'(T)$ and $\tan\delta(T)$ characteristics in the range of the cubic paraelectric phase apart from the above shown anomalies in the surroundings of $F_O - F_T$ and $F_T - P_C$ phase transitions. These additional anomalies and their low frequency dispersion are shown in Figs 7a and b for ceramics sintered for $t_S = 1$ and 7 h, respectively. Such behaviour of the mentioned characteristics was often found in ceramics of perovskite structure [18–20]. The observed anomalies in $\varepsilon'(T)$ and $\tan\delta(T)$ characteristics originate from the occurrence of polar micro regions associated with the non-homogeneous distribution of ion defects. These polar

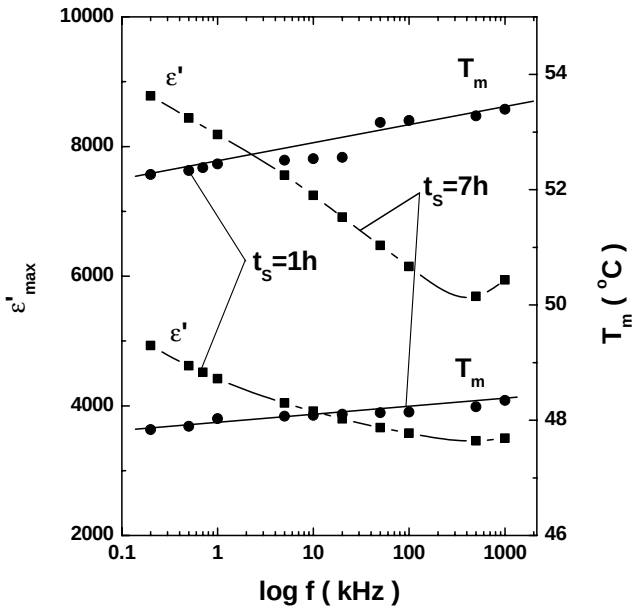

Fig. 6. The maxima in $\varepsilon'(T)$ curves and corresponding temperatures T_m as a function of frequency of measuring field for ceramics with different sintering time t_S.

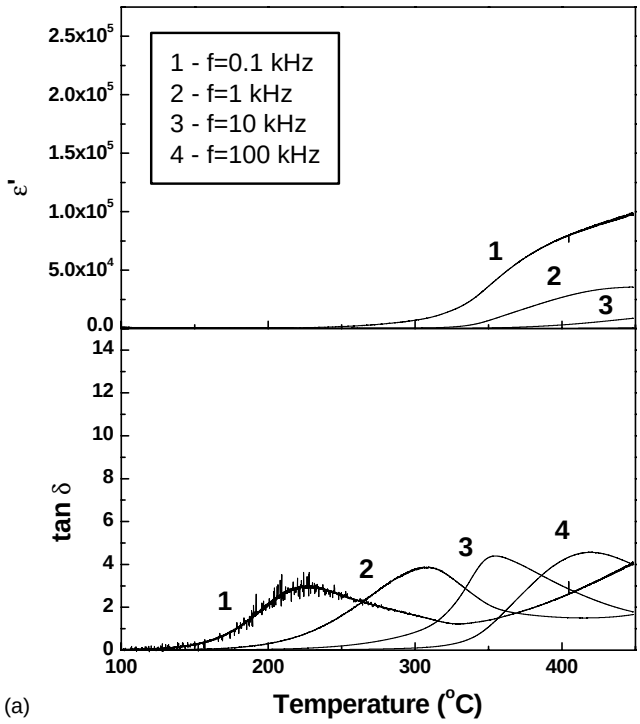

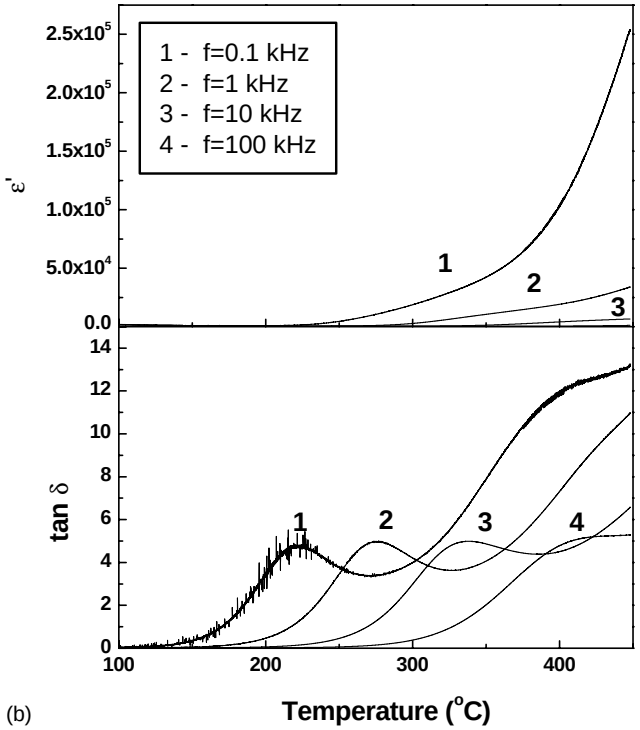

Fig. 7. Temperature dependence of ε' and $\tan\delta$ measured in the range of paraelectric phase at frequencies from 0.1 to 100 kHz for ceramics sintered for $t_S = 1\,h$ (a) and $t_S = 7\,h$ (b).

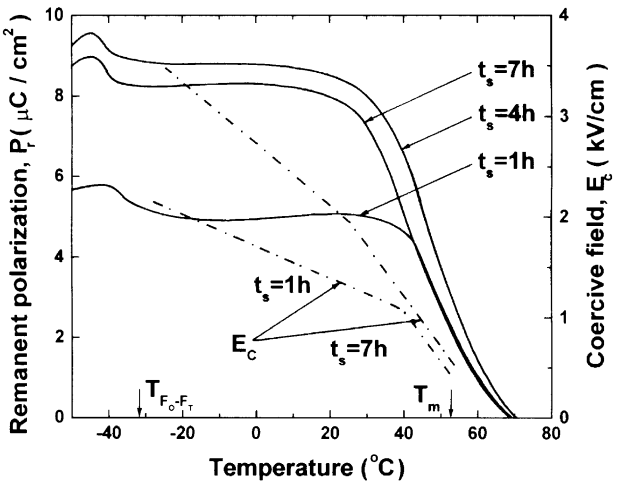

Fig. 8. Remanent polarization and coercive field vs. temperature obtained from hysteresis loop measurements, for ceramics with different sintering time t_S.

micro regions are the traces of non-randomly distributed space charges, previously participating in the screening of FE domains [20].

The occurrence of the above mentioned polar micro regions and their interaction with free electron and ion space charges can also be identified by thermally stimulated depolarization current (TSDC) studies. Such studies, reported in our previous papers [20–22] for other ferroelectric materials, were also performed for the BST ceramics. The obtained results are the subject of our separate paper in preparation [23]. The distinct correlation between wide maxima in TSDC, anomalies in $\varepsilon'(T)$ and $\tan\delta(T)$ characteristics occurring in the range of the paraelectric phase was confirmed.

Remanent polarization (P_r) as a function of temperature was determined from the hysteresis loop measurements. Hysteresis loops were measured at a field of frequency of 50 Hz and of strength 10 kV/cm, using the modified Sawyer–Tower method. The temperature dependence of P_r and the coercive field (E_C) obtained on heating for the ceramics with different sintering times t_S is shown in Fig. 8. The course of the $P_r(T)$ curves differs markedly from the one observed in the vicinity of the normal ferroelectric phase transition particularly, in a wide temperature range in the neighbourhood of temperatures T_m, corresponding to the maxima in $\varepsilon'(T)$ curves (ferroelectric–paraelectric phase transition) (Fig. 3). All the investigated ceramics show relatively small values of the remnant polarization (from 5 to 9 μC/cm^2) at room temperature. The $P_r(T)$ curves show a steep decrease of P_r in the vicinity of the $F_T - P_C$ phase transition temperature. The measurable from hysteresis loops remnant polarization disappears at a temperature considerably higher than T_m. The coercive field (E_C) decreases linearly on heating for all the investigated ceramics. Its values differ considerably for the ceramics obtained for different sintering times (see examples for $t_S = 1$ h and $t_S = 7$ h, shown in Fig. 8).

4. Summary

The experimental data presented above show that an appropriate selection of sintering conditions, and in particular of sintering time, leads to the increase of density of ceramics (Table 1) and to considerable higher values of the dielectric constant (Fig. 3) and the remnant polarization (Fig. 8). It is evidently the result of the increase of the grain size (Table 1 and Fig. 1) and of the crystalline phase content (Fig. 2) in the ceramics. It is obvious that the content of the crystalline and amorphous phases is different in the ceramics with small and large grains. The ε'_{max} and P_r values are lower in the samples containing higher amounts of the amorphous phase within the grain boundaries.

It could be assumed that the lowering of temperature T_m with the increase in the grain size was caused by the change of Sr content within the grains of various sizes (Fig. 4). The EDS analysis excluded, however, this assumption and it is why some other reasons of such behaviour of T_m versus the sintering time should be taken into consideration. In our opinion, the local mechanical stress within the crystal grains and the macroscopic stress within the studied ceramics could be assumed as the main factors that are responsible for the lowering of T_m when the grain size increases. It is known [12] that the resultant mechanical stress is different in the ceramics with grains of small and large sizes due to the difference in the mutual compensation of the stress in the neighbouring grains. This compensation is more complete in the small-grained ceramics. This mechanism, relating among others to $BaTiO_3$ ceramics, is discussed in detail in ref. [12].

The BST 80/20 ceramics obtained at different sintering times, show a strongly diffused ferroelectric phase transition and a deviation from the Curie–Weiss law (Fig. 3). Only weak symptoms of the behaviour typical for ferroelectric relaxors can be noticed (Figs. 5 and 6). The values of the diffuseness exponent $1.118 < \gamma < 1.135$ show that the compositional fluctuations, considered within the framework of Smolensky's interpretation model, are not responsible for the observed deviation from the Curie–Weiss law. Hence, to understand the diffuse character of phase transition around T_m and the observed distinct dispersion of ε' in the high temperature range of the paraelectric phase (Figs. 5 and 7), it is necessary to consider the influence of other internal factors except the above mentioned internal mechanical stress. In our opinion, the occurrence of the ion and electron space charges associated with ion defects, and in particular the oxygen vacancies, should be taken into consideration when interpreting behaviour of the dielectric characteristics. The possible non-homogeneous distribution of the space charge assembling on the various interfaces should be taken into account. These free charges participate in the screening process of the spontaneous polarization, in part of the domains and grains, particularly in those situated in the surface layers of the ceramics and grains. The pinning effect excludes a number of domains from the reversal process and causes a decrease of the remnant polarization determined from

hysteresis loop measurements (Fig. 8). The influence of the internal bias electric field, associated with the space charge polarization in the interfaces causes the increase of the local Curie temperature in a certain part of domains and grains.

Both above discussed factors (an internal mechanical stress and an internal electric field) play a very important role in the behaviour of the investigated ceramics but the macroscopic dielectric characteristics, diffused character of the phase transition and the behaviour of T_m versus grain size are dependent on predomination of one of them. This allow to understand the fact that in small-grained BST 80/20 ceramics (size below 2 μm) the temperature T_m rises [5,6] while this temperature decreases when the average grain sizes increase (the present paper).

References

[1] U. Syamaprasad, R.K. Galgali, B.C. Mohanty, Dielectric properties of the $Ba_{1-x}Sr_xTiO_3$ system, Mater. Lett. 7 (1988) 197–200.

[2] V.V. Lemanov, E.P. Smirnova, P. P Syrnikov, E.A. Tarakanov, Phase transitions and glasslike behaviour in $Sr_{1-x}Ba_xTiO_3$, Phys. Rev. B 54 (1996) 3151–3157.

[3] R. Wang, Y. Inaguma, M. Itoh, Dielectric properties and phase transition mechanisms in $Sr_{1-x}Ba_xTiO_3$ solid solution at low doping concentration, Mater. Res. Bull. 36 (2001) 1693–1701.

[4] V.S. Tiwari, N. Singh, D. Pandey, Diffuse ferroelectric transition and relaxational dipolar freezing in (Ba, Sr)TiO_3, J. Phys. Condens. Matter 7 (1995) 1441–1460.

[5] L. Zhang, W.L. Zhong, C.L. Wang, P.L. Zhang, Y.G. Wang, Dielectric properties of $Ba_{0.7}Sr_{0.3}TiO_3$ ceramics with different grain size, Phys. Stat. Sol. A 168 (1998) 543–548.

[6] L. Zhang, W.L. Zhong, C.L. Wang, P.L. Zhang, Y.G. Wang, Finite-size effects in ferroelectric solid solution $Ba_xSr_{1-x}TiO_3$, J. Phys. D: Appl. Phys. 32 (1999) 546–551.

[7] J.M. Siqueiros, J. Portelles, S. Garcia, M. Xiao, S. Aguilera, Study by hysteresis measurements of the influence of grain size on the dielectric properties of ceramics of the $Sr_{0.4}Ba_{0.6}TiO_3$ type prepared under different sintering conditions, Solid State Commun. 112 (1999) 189–194.

[8] Z. Jiwei, Y. Xi, C. Xiaogang, Z. Liangying, H. Chen, Dielectric properties under dc-bias field of $Ba_{0.6}Sr_{0.4}TiO_3$ with various grain sizes, Mater. Sci. Eng. B 94 (2002) 164–169.

[9] J.H. Yoo, W. Gao, K.H. Yoon, Pyroelectric and dielectric bolometer properties of Sr modified $BaTiO_3$ ceramics, J. Mater. Sci. 34 (1999) 5361–5369.

[10] L. Zhang, W.L. Zhong, C.L. Wang, P.L. Zhang, Y.G. Wang, Dielectric relaxation in barium strontium titanate, Solid State Commun. 107 (1998) 769–773.

[11] J.F. Berton, B. Roelandt, Influence of the sintering parameters on the electrical properties of a high dielectric constant dielectric ceramic, Bull. Soc. Fr. Ceram. 94 (1972) 51–66.

[12] H.T. Martirena, J.C. Burfoot, Grain-size effects on properties of some ferroelectric ceramics, J. Phys. C.: Solid State Phys. 7 (1974) 3182–3192.

[13] S. Chattopadhyay, P. Ayyub, V.R. Palkar, M. Multani, Size-induced diffuse phase transition in the nanocrystalline ferroelectric $PbTiO_3$, Phys. Rev. B 52 (1995) 13177–13183.

[14] S. Chattopadhyay, P. Ayyub, V.R. Palkar, A.V. Gurjar, R.M. Wankar, M. Multani, Finite-size effects in antiferroelectric $PbZrO_3$ nanoparticles, J. Phys.: Condens. Matter 9 (1997) 8135–8145.

[15] W. Luan, L. Gao, J. Guo, Size effect on dielectric properties of fine-grained $BaTiO_3$ ceramics, Ceram. Int. 25 (1999) 727–729.

[16] Y.G. Wang, W.L. Zhong, P.L. Zhang, Size effects on the Curie temperature of ferroelectric particles, Solid State Commun. 92 (1994) 519–523.

[17] Y.G. Wang, W.L. Zhong, P.L. Zhang, Surface effects and size effects on ferroelectrics with a first-order phase transition, Phys. Rev. B 53 (1996) 11439–11443.

[18] O. Bidault, P. Goux, M. Kchikech, M. Belkaoumi, M. Maglione, Space-charge relaxation in perovskites, Phys. Rev. B 49 (1994) 7868–7873.

[19] M. Maglione, Dielectric relaxation and conductivity in ferroelectric perovskites, Ferroelectrics 176 (1996) 1–6.

[20] J. Hañderek, Z. Ujma, C. Carabatos-Nedelec, G. Kugel, D. Dmytrów, I. El-Harrad, Dielectric, pyroelectric, and thermally stimulated depolarization current investigations on lead-lanthanum zirconate-titanate-*x*/95/5 ceramics with La content x= 0.5%–4%, J. Appl. Phys. 73 (1993) 367–373.

[21] Z. Ujma, M. Adamczyk, J. Hañderek, Relaxor properties of $(Pb_{0.75}Ba_{0.25})(Zr_{0.70}Ti_{0.30})O_3$ ceramics, J. Eur. Ceram. Soc. 18 (1998) 2201–2207.

[22] J. Hañderek, M. Adamczyk, Z. Ujma, Dielectric and pyroelectric properties of $(Pb_{1-x}Ba_x)(Zr_{0.70}Ti_{0.30})O_3$ [$x = 0.25 \div 0.35$] ceramics exhibiting the relaxor ferroelectrics behaviour, Ferroelectrics 233 (1999) 253–270.

[23] L. Szymczak, Z. Ujma, J. Hañderek, Pyroelectric and thermally stimulated depolarization current investigations on (Ba,Sr)Ti O_3 ceramics, in preparation.